Tight bounds on thermalization timescales of scarred eigenstates in nonintegrable perturbed Hamiltonian systems

Purpose: **PHYS 2430 Final Project**
Professor: Brad Marston

Introduction: Scarred States

The existence of long-lived low energy excitations (dubbed quasiparticles [4]) of quantum many-body spectra has lend itself a remarkable phenomenon in condensed matter physics [1,2,3,4]. Higher-energy quasiparticles of low decay rates also occur in noninteracting systems ([5,6]) and in some interacting integrable models ([7,8]).
Rendering all of the aforementioned subjects as somewhat classified, esteemed condensed matter physicists have shifted their attention towards understanding long-lived high energy quasiparticles in nonintegrable interacting systems. One such protocol has been named **quantum many-body scars**.
Quantum many-body scars are highly nonthermal eigenstates of a quantum matter system (satisfying the eigenstate thermalization hypothesis [16]) with increased probabilistic weights ([4], [9]). Only a portion of these states represent stable qusiparticles with low decay rates.

1 Introduction: Project Outline

Is there a tight bound on the thermalization timescale for an exact scarred eigenstate of the one-dimensional constrained BH model [22,23]?
In this paper we present a tight bound on the termalization timescale of the exact scarred eigenstate of the nonintegrable constrained 1D Bose-Hubbard Hamiltonian [2,4]. A loose bound on the general thermalization timescale of scarred eigenstates of nonintegrable Hamiltonians was recently found using Lieb-Robinson bounds [11, 18]. It was discovered that the thermalization time is lower-bounded by $T_{th} \sim O(\lambda^{-1/(1+d)})$, where d is the spatial dimension of the system. The paper [11] specifically mentions that the thermalization timescale bound is quite general, likely to be improved in certain models. Hence, the main goal of this paper will be to explore a quantum scarred state in a model that allows for a rigid thermalization time bound.
While there is no shortage of papers discussing thermalization timescales of condensed matter systems, two articles that have proven themselves to be highly useful for exploring the questions above are [12] and [17]. In both papers, for a certain general class of models, narrow exponential bounds resembling the Lieb-Robinson bounds are explored. Finally, in paper [22], it is shown that the Lieb-Robinson bound can be reduced in the case of locally interacting systems. In such frameworks, the corresponding LR "velocity" grows much slower than the original bound with the increase of the number of spatial dimensions of the model D.

This paper is organized as follows:

1. In the section **Background**, we present a sophisticated mathematical tool for deriving (improved) Lieb-Robinson bounds in lattice systems: *the commutativity diagram* [22]. We derive the Lieb-Robinson operator commutator expression [18].
2. Section **Methods** is divided into three chapters. First, we analyze the one-dimensional Bose-Hubbard model. We compute a bound on the information transmission speed in this system using techniques from [22]. In the next section, we consider the Bose-Hubbard chain with a maximum lattice site occupancy of **2** [23,26]. Using results from the previous section, we successfully speculate the LR bound in the constrained model. Finally, we introduce scarred states in the constrained BH model, and make several predictions on (pre)thermalization timescales of such scales.
3. In the section **Discussion**, we study the implications of our thermalization timescale speculations and comoputations and relate such to current research trends.
4. Finally, we propose a number of uncertainties related to the project computations, and relate the reader to useful articles that perhaps contain resolutions to these dilemmas. We outline key takeaways from the project, and suggest possible research questions.

2 Background:Lieb-Robinson Bounds

2.1 Lieb-Robinson Bounds

In [18], Lieb and Robinson investigated the dynamics of general lattice models. The main result of their study is a conclusive bound on thermalization timescales of preconditioned quantum states [11,18,25].
More concretely, let our system be defined on a d-dimensional lattice with a Hamiltonian $\mathcal{H}$. Denote the lattice as Γ. Suppose A, B are observables defined on two finitely distanced regions X, Y [27]. Then for any given time, the following holds [18,22]:

$$||[A_X(t), B_Y(0)]|| \leq C \cdot e^{-\frac{d(X,Y)}{\xi}} \cdot (e^{\frac{Vt}{\xi}} - 1) \tag{1}$$

where $d(X,Y) = inf\{d(x,y)|x \in X, y \in Y\} > 0$ [27], $A_X(t) = e^{iHt} A_X(0) e^{-iHt}$, and ξ, V are constants dependent only on the system Hamiltonian. In particular, V is often referred to as the LR-velocity [22]. It is the speed of information propagation inside the lattice channels.

2.2 The Commutativity Graph

A novel tool that can be defined is the notion of a *commutativity diagram* [22]. It is a graphical representation of the commutation relations of all the Hamiltonian terms.
More rigorously, let us consider a locally interacting quantum system with a Hamiltonian [33]:

$$H = \sum_i h_i \gamma_i \tag{2}$$

where γ_i are all local Hermitian operators of unit norm, and h_i are scalar parameters, and the sum over i's does not necessarilly run over some lattice, but is rather just a sum over a certain countable set, barring nothing but mathematical structure. We construct the following graph:

1. We associate a vertex of the graph to each i, and denote its *weight* to be h_i.
2. Vertices i, j will be connected by an edge in the commutativity graph iff $[\gamma_i, \gamma_j] \neq 0$.

Examples of commutativity graphs can be found in **Section 3** of this paper.
In terms of quantum dynamics, thermalization of the system takes place on the commutativity graph. This intuitive statement needs mathematical rigour, and is hence explored in the next sections. [22]

2.3 Derivation of the Lieb-Robinson bound

The goal of this section is to arrive at an expression for the evolution of the commutator of two operators A, B defined on two finitely distanced sets X, Y. Once again we consider our generalized lattice Hamiltonian [33]:

$$H = \sum_i h_i \gamma_i \tag{3}$$

Instead of immediately dealing with the operator A_X like in (1), we first look at γ_i for a particular lattice site in X. We know the evolution equation for γ_i is [2]:

$$i\frac{d}{dt}\gamma_i(t) = [\gamma_i(t), H] = \sum_{j:<ij>\in E(G)} h_j[\gamma_i(t), \gamma_j(t)] \tag{4}$$

where $E(G)$ is the set of edges of the lattice Γ. Defining $\gamma_i^B(t) = [\gamma_i(t), B(0)]$ [34]:

$$\frac{d}{dt}\gamma_i^B(t) = [\dot{\gamma}_i(t), B(0)] = [\sum_{j:<ij>\in E(G)} h_j[\gamma_i(t), \gamma_j(t)], B(0)] \tag{5}$$

Using the Jacobi identity [30]

$$\frac{d}{dt}\gamma_i^B = [\sum_{j:<ij>\in E(G)} h_j[\gamma_i(t), \gamma_j(t)], B(0)] = \sum_{j:<ij>\in E(G)} hj(\gamma_i(t)[\gamma_j(t), B(0)] + \gamma_j(t)[B(0), \gamma_i(t)] \tag{6}$$

$$\frac{d}{dt}\gamma_i^B = \sum_{j:<ij>\in E(G)} h_j([\gamma_i(t), \gamma_j^B(t)] + [\gamma_j(t), \gamma_i^B(t)]) \tag{7}$$

After several algebraic manipulations of (6), one obtains [22]:

$$||\gamma_i^B(t)|| - ||\gamma_i^B(0)|| = \int_0^t || \sum_{j:<ij>\in E(G)} h_j[\gamma_i(t'), \gamma_j^B(t')]||dt' \leq 2 \cdot \int_0^t \sum_{j:<ij>\in E(G)} ||h_j|| \cdot [\gamma_j^B(t')]||dt' \tag{8}$$

Now we are ready to extend our analysis to an arbitrary operator A with compact support on X, while B has compact support on Y: Let $A(0) = \sum_X h_i\gamma_i$, $B(0) = \sum_Y h_i\gamma_i$. Then [22]:

$$||[A_X(t), B_Y(0)]|| - ||[A_X(0), B_Y(0)]|| \leq \int_0^t \sum_{i\in S(A)} 2||A|| \cdot |hi| \cdot \bar{\gamma}_i^B(t')dt' \tag{9}$$

where $S(A) = \{i : [\gamma_i(0), A(0) \neq 0]\}$, and the function $\bar{\gamma}_i^B(t)$ is given by the evolution equation of $\bar{\gamma}_i^B$ is:

$$\bar{\gamma}_i^B(0) = ||[\gamma_i(0), B(0)]||, \ \frac{d}{dt}\bar{\gamma}_i^B = 2 \cdot \sum_{j:<ij>\in E(G)} |h_i|\bar{\gamma}_i^B(t) \tag{10}$$

By defining

$$H_{ij} = 2\sqrt{|h_i||h_j|} \tag{11}$$

for $ij \in E(G)$ and the following Green's function evolution equation [22]:

$$\frac{d}{dt}G_{ij}(t) = \sum_{k:<ik>\in E(G)} H_{ik}G_{kj}(t) \tag{12}$$

with the initial condition $G_{ij}(0) = \delta_{ij}$.
After plugging in (11) into (8), one obtains [22]:

$$||[A_X(t), B_Y(0)]|| - ||[A_X(0), B_Y(0)]|| \leq 2||A|| \cdot ||B|| \int_0^t \sum_{i\in X, j\in Y} H_{ij}G_{ij}(t')dt' \tag{13}$$

which a remarkable result on its own. One should notice that (12) is highly dependent on the H_{ij} indices. Indeed, using only the commutativity structure of (2) and scalar parameters h_i, one can obtain the timescale necessary for two quantum operators to become correlated. Furthermore, suppose the commutativity graph is described as a lattice of translationally invariant primitive cells labeled by $(n_1, n_2, ...n_d)$, and with an additional index denoting the vertex inside the primitive cell α. Such a philosophy resembles Felix Bloch's treatment of solid state systems [2]. In such conditions, we can write

$$H_{ij} = H_{\alpha\beta}^{mn} \tag{14}$$

with $m = (m_1, m_2, ...m_d)$ and $n = (n_1, n_2, ...n_d)$ denoting indices of primitive cells and α,β representing specific vertices inside one unit cell. The trick lies in the following [33]: Fourier-transform (13) along the lattice described by indices $(n_1, ...n_d)$, but we keep the unit cell indices α,β to attain the transform $H_{\alpha\beta)}^{(\vec{k}}$. Then we plug this transform into (11) to obtain:

$$\frac{d}{dt}G_{\alpha\beta}^{\vec{k}}(t) = \sum_{\gamma} H_{\alpha\gamma}^{\vec{k}}G_{\gamma\beta}^{\vec{k}}(t) \tag{15}$$

After transforming (14) back to real space after letting $G_{\alpha\beta}^{\vec{k}}(t)$ evolve in time, using several complex analysis tools [22,27], we end up with:

$$|G(\vec{r}, t)| \leq c_{\kappa_0} e^{\omega_m(i\kappa_0)t - \kappa_0|\vec{r}|} \tag{16}$$

where $\omega_m(i\kappa_0)$ is the eigenvalue of the matrix $H^{(i\vec{\kappa_0})}$ with maximum modulus, and κ_0 is *any* positive real number. By comparing (15) to (1), it is straightforward to conclude [22]

$$v_{LR} \leq \min_{\kappa_0>0} \frac{\omega_m(\kappa_0)}{\kappa_0} \tag{17}$$

The beauty of the results in [22] lies in (16). There exists a successful recipe for obtaining improved Lieb-Robinson bounds in discete quantum systems:

1. Describe the commutativity diagram of (2). Specifically, we are interested in the lattice structure of the commutativity diagram.
2. Compute entries of $H_{ij} = 2\sqrt{|h_i||h_j|}$ (10), and Fourier transform H_{ij} along the commutativity graph sublattice to attain $H^{(\vec{k})}$ like in (14).
3. Find the largest eigenvalue of $H^{(i\vec{k})}$.
4. Estimate $v_{LR} \leq \min_{\kappa_0>0} \frac{\omega_m(\kappa_0)}{\kappa_0}$

3 Methods: The LR velocity of the Bose-Hubbard chain

3.1 The Bose-Hubbard Chain

In the following section we compute the improved the Lieb-Robinson velocity bound for the one-dimensional Bose-Hubbard model. A general analysis of such a bound was covered in [22], in the context of $su(n)$ Fermi-Hubbard models [35]. However, the author of the article is not aware of any scientific literature that uses tools from [22] to compute the improved Lieb-Robinson bounds of the BH chain.
The Hamiltonian for the Bose-Hubbard model on a 1D chain is [2]:

$$H_0 = -J\sum_i b_i^\dagger b_{i+1} + b_i b_{i+1}^\dagger \tag{18}$$

$$H_{int} = U\sum_i n_i(n_i - 1)$$

We turn off the interactions first, and try to construct the commutativity diagram of the interaction-free Bose-Hubbard chain:
We have the following commutation relations

$$[b_i, b_j^\dagger] = \delta_{ij},\ [b_i, b_j] = 0 \tag{19}$$

for all i, j. Hence

$$[b_i^\dagger b_{i+1} + b_i b_{i+1}^\dagger, b_{i+1}^\dagger b_{i+2} + b_{i+1} b_{i+2}^\dagger] = b_i^\dagger b_{i+2} - b_i b_{i+2}^\dagger \neq 0 \tag{20}$$

For all i. On the other hand,

$$[b_i^\dagger b_j + b_i b_{i+1}^\dagger, b_i^\dagger b_j + b_i b_j^\dagger] = 0 \tag{21}$$

for $j \geq i+2$.
So the commutativity diagram of the free Bose-Hubbard chain has the following depiction:

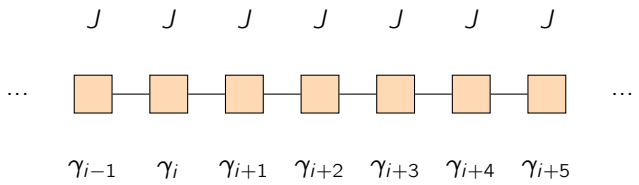

Figure 1: The Commutativity graph of the interaction-free Bose-Hubbard chain: $\gamma_i = b_i^\dagger b_{i+1} + b_i b_{i+1}^\dagger$

We can immediately compute the matrix H_{ij} for (18): we note that a primitive unit cell is trivial in this model;

$$H_{ij} = 2J(\delta_{i,j+1} + \delta_{i,j-1}) \tag{22}$$

We now take the Fourier transform of H_{ij}:

$$H^{(k)} = 2J(e^{ika} + e^{-ika}) \tag{23}$$

where a is the lattice constant.
Clearly,

$$\omega_m(ik) = 2J(e^{-ka} + e^{ka}) \tag{24}$$

And therefore

$$V_{LR} \leq \min_{\kappa>0} \frac{2J(e^{-\kappa a} + e^{+\kappa a})}{\kappa} = 2X_0 Ja \tag{25}$$

where $X_0 = \min\{(e^{-x} + e^x)/x\}$ over $x > 0$, and $X_0 \approx 3,018$.
We now turn on interactions, so that we have

$$H = \sum_i -Jb_i^\dagger b_{i+1} + \sum_i -Jb_i b_{i+1}^\dagger + \sum_i Un_i(n_i - 1) \tag{26}$$

with an additional relation

$$[n_i(n_i - 1), b_i^\dagger b_{i+1}] \neq 0 \tag{27}$$

because if we first shift a particle by a lattice site, and then apply the number operator on the abandoned site, we get a different effect than when first measuring the number of particles at a given site and then shifting them.
So the commutativity diagram of the model has additional structure, as is demonstrated in the following graph:

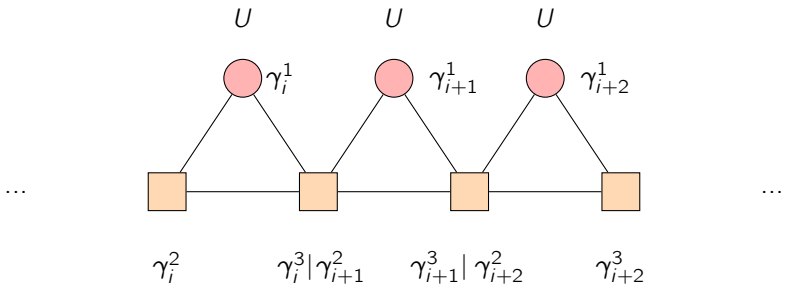

Figure 2: Commutativity Graph of the Bose-Hubbard Chain with Interactions:
$\gamma_i^1 = n_i(n_i-1)$, $\gamma_i^2 = -b_i b_{i+1}^\dagger$, $\gamma_i^3 = -b_i^\dagger b_{i+1}$

We see that the commutativity graph of the full model (18) is actually a chain of triangular primitive unit cells. Just as before, we can construct the $H_{\alpha\beta}^{ij}$ matrix:

$$H_{ij} = 2\begin{pmatrix} 0 & J(\delta_{i,j+1}+\delta_{i,j-1}) & \sqrt{JU}\delta_{ij} \\ J(\delta_{i,j+1}+\delta_{i,j-1}) & 0 & \sqrt{JU}\delta_{ij} \\ \sqrt{JU}\delta_{ij} & \sqrt{JU}\delta_{ij} & 0 \end{pmatrix} \tag{28}$$

After Fourier-transforming (28), just like in (15), we obtain:

$$H_{\alpha\beta}^{k} = 2\begin{pmatrix} 0 & J(e^{ika}+e^{-ika}) & \sqrt{JU} \\ J(e^{ika}+e^{-ika}) & 0 & \sqrt{JU} \\ \sqrt{JU} & \sqrt{JU} & 0 \end{pmatrix} \tag{29}$$

After computing the largest eigenvalue of (29), we attain

$$\omega_m(i\kappa) = 2J\cosh\kappa a + 2\sqrt{4JU + J^2\cosh^2\kappa a} \tag{30}$$

We can write (29) in a more compact form, by introducing the interaction factor $u = U/J$:

$$\omega_m(i\kappa) = 2J(\cosh\kappa a + \sqrt{4u+\cosh^2\kappa a}) \tag{31}$$

We immediately see that if we turn off interactions, we obtain (24). From (31) we obtain the LR bound for the BH chain with interactions:

$$V_{LR} \leq = 2Ja \cdot \min_{x>0} \frac{\cosh x + \sqrt{4u+\cosh^2 x}}{x} \tag{32}$$

Let us plot (32):

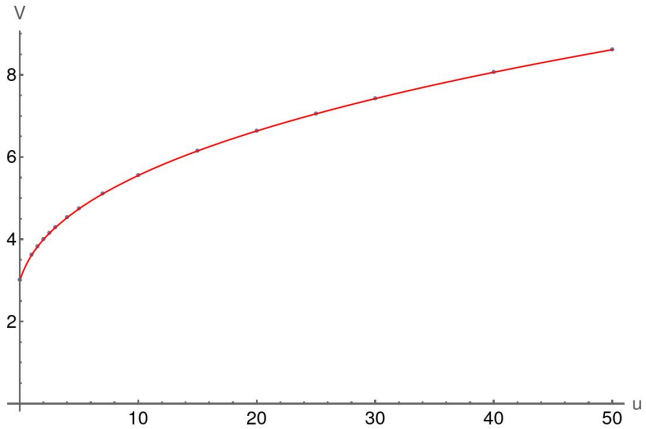

Figure 3: *Lieb-Robinson velocity bound of the interacting BH chain versus the interaction factor* u

We see that the bound on V_{LR} grows logarithmically fast as we turn on the interactions in the system. This is telling us that, even when $u \sim 1$, we can get a reasonably tight bound on the information propagation velocity in the system.

4 Methods: The Constrained Bose-Hubbard model

A close relative of the one-dimensional Bose-Hubbard model, the constrained BH chain has the Hilbert space of the original chain restricted to the maximal occupancy of every lattice site being some $n_{\max}$ [23]. From now on, we will be working with $n_{\max} = 2$. We form the constrained Hamiltonian by using the projection operator $P_{n\leq 2}$ on both sides of the Hamiltonian:

$$H_{\text{constrained}} = P_{n\leq 2} \cdot H \cdot P_{n\leq 2} \tag{33}$$

which becomes [23]:

$$H_0' = J\sum_i a_i^\dagger a_{i+1} + a_i a_{i+1}^\dagger \tag{34}$$

$$H_{\text{int}}' = U\sum_i \nu_i(\nu_i - 1)$$

where $a_i = P_{n\leq 2} b_i P_{n\leq 2}$, and $\nu_i = a_i^\dagger a_i$. Operators $a_i, a_j^\dagger$ now satisfy a nontrivial algebra. Namely, it can be shown that [23]:

$$[(a_i)^2, (a_j^\dagger)^2] = (2 - 2a_i^\dagger a_i)\delta_{ij} \tag{35}$$

$$[a_i^\dagger a_i, (a_j^\dagger)^2] = 2(a_i^\dagger)^2 \delta_{ij} \tag{36}$$

Full understanding of commutation relations in (33) remains a great challenge to this day [13,19,23]. However, we notice that the *commutativity diagram* of this system retains the **same structure** as the commutativity diagram of (18). This is because the new commutation relations between any two operators $\gamma_i^\alpha, \gamma_j^\beta$ in the 1D Bose-Hubbard model map as follows:

$$[\gamma_i^\alpha, \gamma_j^\beta] \to [P\gamma_i^\alpha P, P\gamma_j^\beta P] = P[\gamma_i^\alpha, \gamma_j^\beta]P \tag{37}$$

where we denote $P_{n_{max}=2}$ as P. Now we notice that if $[\gamma_i^\alpha, \gamma_j^\beta] = 0$, then $P[\gamma_i^\alpha, \gamma_j^\beta]P = 0$, and $[\gamma_i^\alpha, \gamma_j^\beta] \neq 0$ implies $P[\gamma_i^\alpha, \gamma_j^\beta]P \neq 0$.
Because the commutativity diagram of (33) has the same structure as the commutativity diagram of (18), we immediately inherit a bound on the speed of information propagation inside the constrained Bose-Hubbard channels:

$$V_{LR} \leq 2Ja \cdot f(u) \tag{38}$$

where $f(u) = \min_{x>0} \frac{\cosh x + \sqrt{4u + \cosh^2 x}}{x}$ is the previously derived interaction-dependent function in (32).

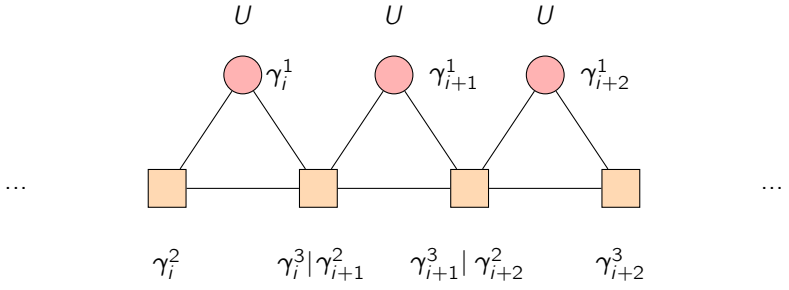

Figure 4: The Commutativity graph of the Bose-Hubbard chain with interactions; The gamma-operators in this case are $\gamma_i^1 = \nu_i(\nu_i - 1)$, $\gamma_i^2 = a_i a_{i+1}^\dagger$, $\gamma_i^3 = -a_i^\dagger a_{i+1}$

5 Methods: Scarred State Thermalization in CBH

Model (33) has a *scarred state* [4]: a long-lived quasiparticle state. While a general analysis of the timescale of decay of such a state need not be done using Lieb-Robinson bounds [4, 10, 16, 23], using the tools we have developed so far, it is relatively straightforward to estimate the decay rate of such a state.
We begin by constructing the ladder operators in (33):

$$J^{+} = \sum_{i} \frac{(-1)^{r_i}}{\sqrt{2}} a_i^2, \;\; J^{-} = J^{+\dagger} \tag{39}$$

the scarred state with index n of (33) is then given by [23]

$$|J_n\rangle = (J^{+})^{n} |\Omega\rangle \tag{40}$$

$|\Omega\rangle$ is the projection of the vacuum of the original BH chain under the operator $P_{n\leq 2}$. It is easy to estimate the thermalization timescale of (40): We already have the Lieb-Robinson velocity, so we just need to find the length scale of the scarred state; if the spacial extension of the scarred state is given by L, then the decay rate/thermalization timescale of such a state is given by

$$\tau^{-1} \leq \frac{V_{LR}}{L} \tag{41}$$

With the improved Lieb-Robinson bound on the constrained Bose-Hubbard model in (38), we are likely to find a tight estimation of the decay rate of the scarred state.
Employing quantum mechanical uncertainty relations [2] on (39), the length scale of the scarred state in (39) is given by the inverse momentum scale of the scarred state.
The author is still trying to understand how to use the ladder operators in (39) to estimate the spatial extent of the scarred state. Working with angular momentum operators seems extremely incovinient when it comes to Fourier-transforming (39). At this moment in time, the only insight into the extent of the system is given by data in [23]: It seems like scarred states form periodic spatial structures, but a formula for a period of such patterns is still unclear.

6 Discussion and Conclusive Thoughts

In this paper we made an attempt to understand thermalization timescales of scarred eigenstates of nonintegrable Hamiltonians from the point of view of information propagation timescales in the system: the Lieb-Robinson bounds. Our efforts have lead us to a convenient expression for the LR speed limit in Bose-Hubbard 1D systems. We argued that the LR bound of the Bose-Hubbard chain can be employed in any constrained Bose-Hubbard chain model. We were able to set up a framework for analyzing scarred states in terms of the derived LR velocity bounds, but remained unsuccessful in determining the final relaxation timescale of the Bose-Hubbard system scarred state (39). Our project remained inconclusive in terms of its final product, but the methods we have developed in (18-38) can easily be extended to any system with scarred eigenstates [4,9,16,22, 31,32]. While the constrained BH model is an exotic quantum system, many other models such as the constrained Ising [32], AKLT [13], Haldane-Shastry model [31], which have scarred states, do not have an explicitly computed improved LR velocity bound. Therefore, it would be convenient to develop tools for understanding spacial extensions of scarred states in these models, just as in (41).
Some closing thoughts/questions:

1. What happens to the LR bound as we decrease/increase $n_{\max}$ in (14)? Concretely, is it possible to make an even tighter bound than (38) by varying n_{max}?

2. How does a superposition of two scarred states in (14) thermalize? Again, using the techniques developed in [22], it makes sense to analyze scarred states as a collection of various propagating wave-like excitations in the system. Understanding superposition is always a good proxy for understanding thermalization of a general superposition of quantum states.

3. How does thermalization of the scarred state (40) (in the model (33)) work in the limits $U >> J$, $U << J$? More generally, how does particle interaction affect the scarred state thermalization protocol?

4. In [23], it is speculated that there is a map resembling the Jordan-Wigner [5] (or perhaps the Holstein-Primakoff [2]) transformation that would map the scarred state onto a highly symmetric structure. If such a map exists, it could most definitely be utilized in (41), or maybe even in the main description of the scarred state (39).

References

[1] Goldstone, J (1961). "Field Theories with Superconductor Solutions". Nuovo Cimento. 19 (1): 154–164. Bibcode:1961NCim...19..154G. doi:10.1007/BF02812722. S2CID 120409034.

[2] Coleman, Piers. Introduction to Many Body Physics (PDF). Rutgers University. p. 143. Archived from the original (PDF) on 2012-05-17. Retrieved 2011-02-14. (draft copy)

[3] I. Pomeranchuk (1959). "ON THE STABILITY OF A FERMI LIQUID". Sov. Phys. JETP. 8: 361–362.

[4] Quantum Many-Body Scars: A Quasiparticle Perspective Anushya Chandran, Thomas Iadecola, Vedika Khemani, Roderich Moessner Annual Review of Condensed Matter Physics 2023 14:1, 443-469

[5] Nielsen, Michael (29 July 2005). "The Fermionic canonical commutation relations and the Jordan-Wigner transform" (PDF). futureofmatter.com.

[6] Bethe, H. (March 1931). "Zur Theorie der Metalle. I. Eigenwerte und Eigenfunktionen der linearen Atomkette". Zeitschrift für Physik. 71 (3–4): 205–226. doi:10.1007/BF01341708. S2CID 124225487.

[7] Hubbard, J. (1963). "Electron Correlations in Narrow Energy Bands". Proceedings of the Royal Society of London. 276 (1365): 238–257. Bibcode:1963RSPSA.276..238H. doi:10.1098/rspa.1963.0204. JSTOR 2414761. S2CID 35439962.

[8] Hosur, P. R. (2012). Consequences of non-trivial band topology in condensed matter systems. UC Berkeley.

[9] Turner CJ, Michailidis AA, Abanin DA, Serbyn M, Papic Z. 2018. "Quantum many-body scars" Nat. Phys. 14(7):745–49

[10] Turner, C. J., et al. "Quantum scarred eigenstates in a Rydberg atom chain: Entanglement, breakdown of thermalization, and stability to perturbations." Physical Review B 98.15 (2018): 155134.

[11] Lin CJ, Chandran A, Motrunich "Slow thermalization of exact quantum many-body scar states under perturbations" OI. 2020. Phys. Rev. Res. 2(3):033044

[12] Berislav Buča "Unified Theory of Local Quantum Many-Body Dynamics", Phys. Rev. X 13, 031013 – Published 2 August 2023

[13] Affleck, Ian; Kennedy, Tom; Lieb, Elliott H.; Tasaki, Hal (1987). "Rigorous results on valence-bond ground states in antiferromagnets". Physical Review Letters. 59 (7): 799–802. Bibcode:1987PhRvL..59..799A. doi:10.1103/PhysRevLett.59.799. PMID 10035874.

[14] Shi, Z., Dissanayake, S., Corboz, P. et al. Discovery of quantum phases in the Shastry-Sutherland compound SrCu2(BO3)2 under extreme conditions of field and pressure. Nat Commun 13, 2301 (2022). https://doi.org/10.1038/s41467-022-30036-w

[15] Nussinov, Zohar. "Klein spin model ground states on general lattices." arXiv: Strongly Correlated Electrons (2006): n. pag. arXiv:cond-mat/0606075 [cond-mat.str-el]

[16] Mark Srednicki (1994). "Chaos and Quantum Thermalization". Physical Review E. 50 (2): 888–901. arXiv:cond-mat/9403051v2. Bibcode:1994PhRvE..50..888S. doi:10.1103/PhysRevE.50.888. PMID 9962049. S2CID 16065583.

[17] Francisco Machado, Gregory D. Kahanamoku-Meyer, Dominic V. Else, Chetan Nayak, and Norman Y. Yao Phys. Rev. Research 1, 033202 – Published 24 December 2019

[18] Lieb, Elliott H.; Robinson, Derek W. (1972). "The finite group velocity of quantum spin systems". Communications in Mathematical Physics. Springer Science and Business Media LLC. 28 (3): 251–257. Bibcode:1972CMaPh..28..251L. doi:10.1007/bf01645779. ISSN 0010-3616. MR 0312860. S2CID 122298337.

[19] Gersch, H.; Knollman, G. (1963). "Quantum Cell Model for Bosons". Physical Review. 129 (2): 959. Bibcode:1963PhRv..129..959G. doi:10.1103/PhysRev.129.959.

[20] Michael Levin and Xiao-Gang Wen Phys. Rev. B 73, 035122 – Published 23 January 2006

[21] Brush, Stephen G. (1967). "History of the Lenz-Ising Model". Reviews of Modern Physics. 39 (4): 883–893. Bibcode:1967RvMP...39..883B. doi:10.1103/RevModPhys.39.883.

[22] Zhiyuan Wang and Kaden R.A. Hazzard PRX Quantum 1, 010303 – Published 3 September 2020

[23] R. Kaneko, M. Kunimi and I. Danshita, [arXiv:2308.12151 [cond-mat.quant-gas]].

[24] Deutsch, Joshua M. "Eigenstate thermalization hypothesis." Reports on Progress in Physics 81.8 (2018): 082001.

[25] Scholarpedia Website, http://www.scholarpedia.org/article/Lieb-Robinson-bounds, Accessed Nov 2023

[26] D. A. Roberts and B. Swingle, Phys. Rev. Lett. **117**, no.9, 091602 (2016) doi:10.1103/PhysRevLett.117.091602 [arXiv:1603.09298 [hep-th]].

[27] Browder, Andrew. Mathematical analysis: an introduction. Springer Science, Business Media, 2012.

[28] Bravyi, Sergey, Matthew B. Hastings, and Frank Verstraete. "Lieb-Robinson bounds and the generation of correlations and topological quantum order." Physical review letters 97.5 (2006): 050401.

[29] Sigal, Israel Michael, and Jingxuan Zhang. "On propagation of information in quantum many-body systems." arXiv preprint arXiv:2212.14472 (2022).

[30] M. Srednicki, "Quantum Field Theory", Cambridge University Press, 2007.

[31] F. D. M. Haldane, 'Exact Jastrow-Gutzwiller resonating valence bond ground state of the spin 1/2 antiferromagnetic Heisenberg chain with 1/r 2 exchange' Phys. Rev. Lett. **60**, 635 (1988) doi:10.1103/PhysRevLett.60.635

[32] Aldous, David, and Persi Diaconis. "The Asymmetric One-Dimensional Constrained Ising Model." arXiv preprint math/0110023 (2001).

[33] Hastings, Matthew B. "Locality in quantum systems." Quantum Theory from Small to Large Scales 95 (2010): 171-212.

[34] Bravyi, Sergey, Matthew B. Hastings, and Frank Verstraete. "Lieb-Robinson bounds and the generation of correlations and topological quantum order." Physical review letters 97.5 (2006): 050401.

[35] Stanisic, Stasja, et al. "Observing ground-state properties of the Fermi-Hubbard model using a scalable algorithm on a quantum computer." Nature Communications 13.1 (2022): 5743.